

Supporting information:

Co₃X₈ (X = Cl and Br): multiple phase and magnetic properties in Kagome lattice

Haoyun Bai¹, Zhichao Yu¹, Jinxian Feng¹, Di Liu¹, Weiqi Li² and Hui Pan^{1,3}*

¹ Institute of Applied Physics and Materials Engineering, University of Macau, Macao SAR, 999078, P.R. China

² School of Physics, Harbin Institute of Technology, Harbin 150001, P.R. China

³ Department of Physics and Chemistry, Faculty of Science and Technology, University of Macau, Macao SAR, 999078, P. R. China

*Corresponding Author

H. Pan: huipan@um.edu.mo (email), +853 88224427 (tel.), +853-88222454 (fax)

Supplementary note

1. Confirmation of lattice constants of Co₃X₈ (X = Cl and Br)

To get the stable structures of 12- and 156-Co₃X₈, the full optimizations were firstly carried out. We find that the optimized structure exhibits spontaneous symmetry breaking, which results in different lattice constants ($a \neq b$) and changed lattice angle ($\theta \neq 120^\circ$). Moreover, the magnetic properties of Co₃X₈ are complex during the structure optimization, as the magnetic ground state changes when the lattice changes (Table S4). Thus, we changed the lattice to a hexagonal lattice and redo the optimization. After multiple optimizations, we obtain the energy-optimized lattice constant.

To confirm whether the obtained lattice constants are accurate, the strain-energy fitting was performed. According to the Born-Huang criteria, the strain energy density of 2D material under biaxial strain fits a second-order relationship with strain, that is,

$$U(\varepsilon) = \frac{1}{2}C_{11}\varepsilon^2$$

$$U(a) = U(a_0) + U(\varepsilon)$$

where $U(\varepsilon)$ is the energy change after applying strain, $U(a)$ is the total energy when lattice constant is a , C_{11} is the elastic constant, and ε is biaxial strain, which is defined as

$$\varepsilon = (a - a_0)/a_0$$

where a is lattice constant under strain, and a_0 is the lattice constant in equilibrium. Thus, $U(a)$ and a has a second-order relationship:

$$U(a) = Aa^2 + Ba + C$$

Then, we can obtain the lattice constant in equilibrium:

$$a_0 = \frac{B}{2A}$$

To simulate biaxial strain, a series of lattice constants were set, and lattice-fixed optimization were performed to obtain the stable structure, and the energy of magnetic ground states were used for energy-strain fitting (Figure S2-3). To improve accuracy, we removed points that are not on the fitted curves clearly. The fitting results show that the lattice constants obtained by the multiple optimizations are accurate enough. For example, the lattice constant of 12-Co₃Br₈ is 7.302 Å by DFT, and 7.33 Å by fitting. The error is only 0.36%. Furthermore, we also showed that a weak strain has little effect on the magnetic and electronic properties of Co₃X₈. Thus, the optimized lattice constants were used in the study.

2. The label of different magnetic arrangements

To determine the magnetic ground states of Co₃X₈ (X = Cl and Br), ten kinds of magnetic arrangements are considered in total (as listed in Table S3 & Figure S8). However, some arrangements cannot exist, such as FM in 12-Co₃X₈. We marked the final states of these arrangements in Table S3. For the FM state in 156-Co₃X₈ and 12-Co₃X₈ under strain ($\varepsilon < -6\%$), three Co ions have different magnetic moments, which is different from the magnetic moments in ferromagnetic structures. Specially, the optimized magnetic properties of AFM1, AFM3, and AFM5 arrangements of 12-Co₃X₈ are actually not antiferromagnetic arrangement, as Co2 shows very weak or no magnetic moments (Figure S9), which is different from the definition of AFM. As the total magnetic moments of them are zero, here we still use the original label to refer to their optimized result. For the AFM2 state, the magnetic arrangement changed into a unregular FIM state after the optimization, where two of twelve Co atoms are spin-up only, resulting in a total magnetic moment of $\sim 6 \mu_B$ (Table S3 & Figure S9).

Supporting Tables

Table S1. The lattice parameters (a), thickness (t), total energy (E_0), and formation energy (E_f) of Co_3X_8 (X = Cl and Br).

SG		lattice (Å)		E_0 (eV)	E_f (eV/unitcell)	E_f (eV/atom)
		a	t			
164	Co_3Cl_8	6.755	2.544	-41.421	-5.635	-0.512
	Co_3Br_8	7.148	2.682	-37.154	-2.987	-0.271
	Co_3I_8	7.725	2.928	-33.487	-0.241	-0.022
156	Co_3Cl_8	6.769	2.500	-41.428	-5.642	-0.513
	Co_3Br_8	7.199	2.663	-37.160	-2.993	-0.272
	Co_3I_8	7.710	2.930	-33.492	-0.246	-0.022
12	Co_3Cl_8	6.888	2.500	-41.593	-5.807	-0.528
	Co_3Br_8	7.302	3.066	-37.279	-3.112	-0.282
	Co_3I_8	7.721	2.931	-33.496	-0.250	-0.023

Table S2. The calculated elastic constants of 12- and 156- Co_3X_8 (X = Cl and Br). Unit: (GPa).

	SG	C_{11}	C_{22}	C_{12}	C_{44}
Co_3Cl_8	156	31.934	31.934	9.291	11.322
	12	25.051	22.661	6.846	8.308
Co_3Br_8	156	32.257	32.257	9.378	11.441
	12	22.651	21.074	5.693	7.401

Table S3. The total energy (E_0), energy difference between ground state (ΔE) and magnetic moment (magmom) for different magnetic configurations in a supercell. The magnetic states in “magmom” indicates the final magnetic configuration is changed into different configurations.

156- Co_3X_8						
	Co_3Cl_8			Co_3Br_8		
	E_0 (eV)	ΔE (meV)	magmom (μ_B)	E_0 (eV)	ΔE (meV)	magmom (μ_B)
FM	-165.70	27.47	4	-148.62	33.5	4.0002
FIM	-165.73	0	1.2439	-148.66	0	1.211
NM	-165.35	375.45	0	-148.32	337.02	0
AFM1	-165.62	106.48	0	-148.55	109.72	0.0001
AFM2	-164.93	800.03	0	-148.59	66.15	0
AFM3	-165.57	158.00	0	-148.50	155.85	0
AFM4	-165.69	35.86	-0.0022	-148.62	37.29	0.0643
AMF5	-165.65	78.43	-0.0179	-148.52	132.7	0.0007
FIM-like	-165.65	75.89	0	-148.59	64.51	0

2_only	AFM-like			AFM-like		
12-Co₃X₈						
	Co ₃ Cl ₈			Co ₃ Br ₈		
	E ₀ (eV)	ΔE (meV)	magmom (μ _B)	E ₀ (eV)	ΔE (meV)	magmom (μ _B)
FM			FIM			FIM
FIM	-166.31	67.05	12.000	-148.96	159.96	11.998
NM	-164.15	2224.47	0.001	-147.12	2004.43	0.000
AFM1	-166.34	42.32	0.000	-149.01	104.72	0.000
AFM2	-166.34	33.85	5.7368	-149.01	108.02	5.841
AFM3	-166.27	106.38	0.000	-148.87	248.26	0.000
AFM4			AFM-like			AFM-like
AMF5	-166.37	2.42	0.000	-149.02	103.82	0.000
FIM-like	-166.37	0.00	0.000	-149.12	0.00	0.000
2_only			FIM			NM

Table S4. The energy (eV)-lattice parameter (a) data of AFM-like, FIM FM states when applying biaxial strain on Co₃X₈ (X = Cl and Br), and d₁/d₂ in 12-Co₃X₈. The data in bracket is the energy of FIM-5 state.

a (Å)	12-Co₃Cl₈				156-Co₃Cl₈		
	d₁/d₂	FIM-like	FIM	FM	FIM-like	FIM	FM
6.500	0.975	-41.187	-41.191	-41.188	-41.176	-41.174	-41.186
6.550	0.974	-41.273	-41.277	-41.270	-41.261	-41.274	-41.271
6.600	0.913	-41.307	-41.312	FIM	-41.326	-41.340	-41.335
6.650	0.896	-41.404	-41.389	FIM	-41.373	-41.387	-41.382
6.700	0.889	-41.472	-41.454	FIM	-41.401	-41.416	-41.410
6.800	0.880	-41.559	-41.541	FIM	-41.407	-41.424	-41.417
6.900	0.873	-41.596	-41.579	FIM	-41.355	-41.373	-41.367
7.000	0.865	-41.584	-41.567	FIM	-41.245	-41.269	-41.260
7.050	0.857	-41.561	-41.545	FIM	-41.225	-41.214	-41.186
7.100	0.852	-41.529	-41.512	FIM	-41.181	-41.171	-41.133
7.150	0.848	-41.487	-41.471	FIM	-41.130	-41.140	-41.069
7.200	0.864	-41.413	-41.300	FIM-5 (-41.286)	-41.056	-41.128	-41.003
7.250	0.857	-41.363	-41.244	FIM-5 (-41.237)			
7.300	0.851	-41.304	-41.154	FIM-5 (-41.179)	-40.883	-41.023	-40.876
a (Å)	12-Co₃Br₈				156-Co₃Br₈		
	d₁/d₂	FIM-like	FIM	FM	FIM-like	FIM	FM

6.700	1.023	-36.357	-36.384	-36.383	-36.375	-36.380	-36.383
6.750	1.005	-36.537	-36.546	-36.534	-36.539	-36.544	-36.545
6.800	1.006	-36.678	-36.687	-36.686	-36.682	-36.688	-36.687
7.000	0.978	-37.062	-37.064	FIM	-37.053	-37.062	-37.055
7.050	0.980	-37.108	-37.110	FIM		□	
7.100	0.905	-37.168	-37.138	FIM	-37.134	-37.145	-37.137
7.250	0.890	-37.268	-37.230	FIM	-37.133	-37.146	-37.138
7.350	0.882	-37.279	-37.236	FIM	-37.064	-37.080	-37.072
7.400	0.880	-37.268	-37.224	FIM	-37.012	-37.028	-37.019
7.600	0.864	-37.141	-37.094	FIM	-36.828	-36.906	-36.779
7.650	0.849	-37.089	-37.043	FIM			
7.700	0.871	-37.018	-36.889	FIM-5			
			(-36.927)				
7.800	0.853	-36.898	-36.761	FIM-5	-36.534	-36.681	-36.522
			(-36.807)				

Supporting Figures

Structure, energy fitting and stability

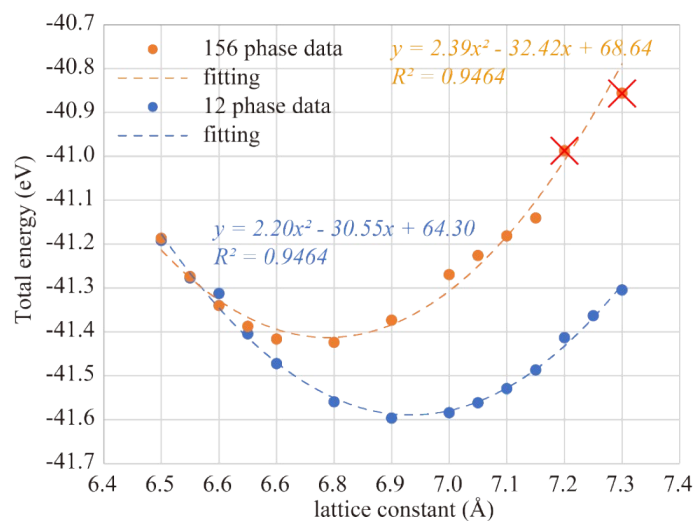


Figure S1. The strain-energy fitting of Co_3Cl_8 . The points marked with a red cross were not used for fitting.

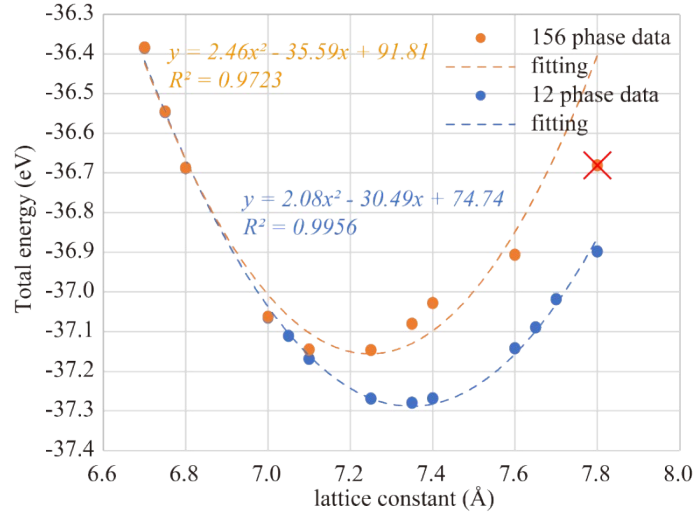


Figure S2. The strain-energy fitting of Co_3Br_8 . The points marked with a red cross were not used for fitting.

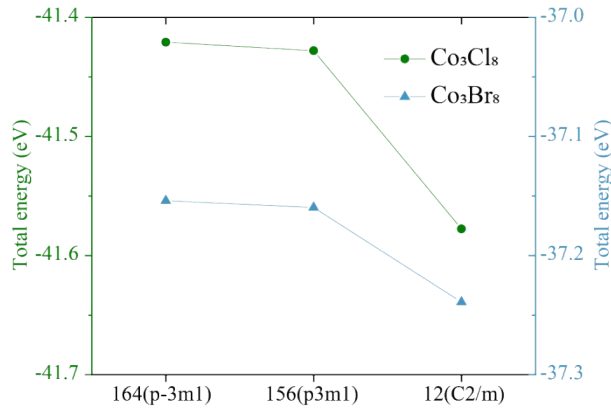


Figure S3. The total energies of Co_3X_8 with different phases.

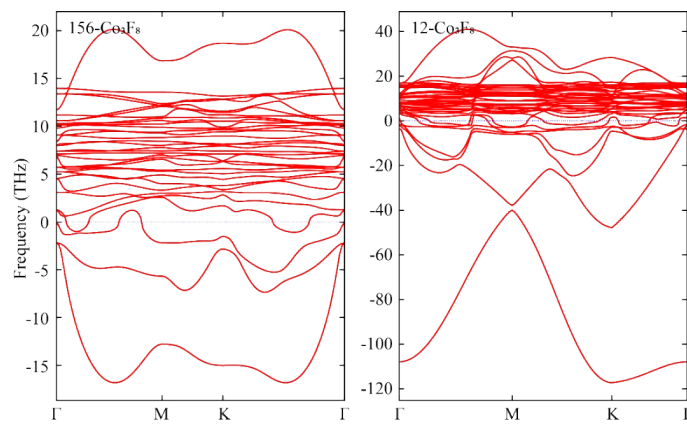


Figure S4. The phonon spectra of $156\text{-Co}_3\text{F}_8$.

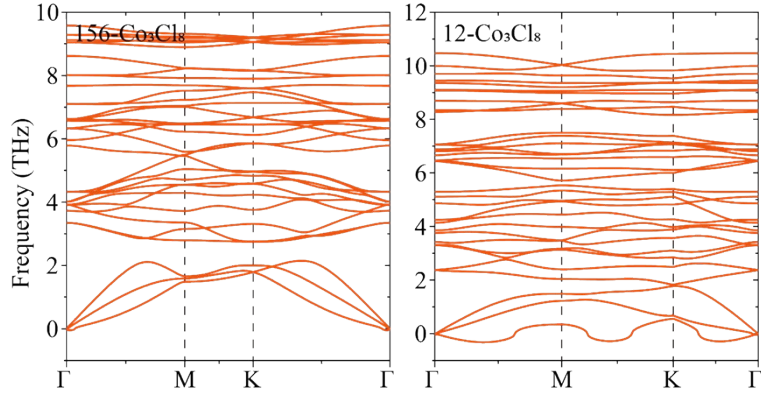


Figure S5. The phonon spectra of Co_3Cl_8 .

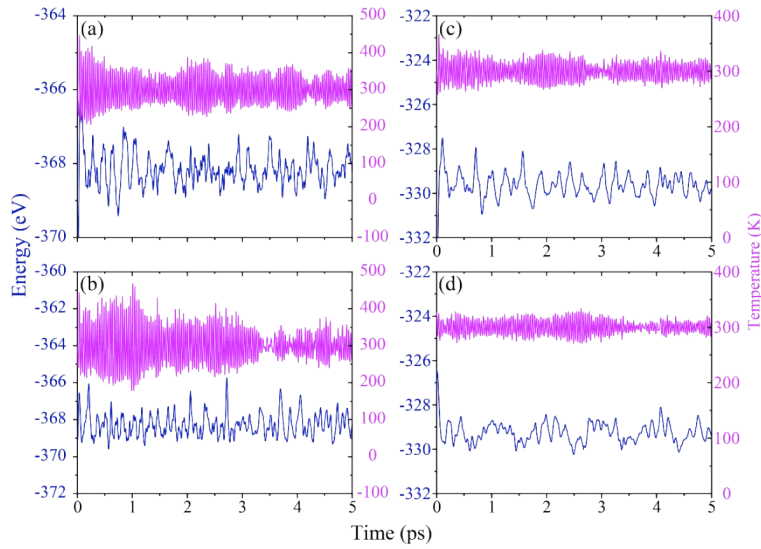


Figure S6. The AIMD simulations of (a) $156\text{-Co}_3\text{Cl}_8$, (b) $12\text{-Co}_3\text{Cl}_8$, (c) $156\text{-Co}_3\text{Br}_8$ and (d) $12\text{-Co}_3\text{Br}_8$.

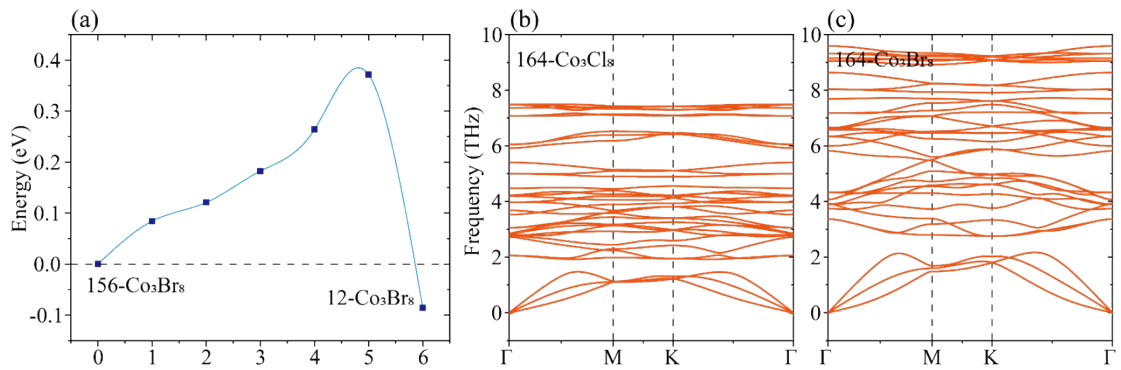


Figure S7. (a) The energy diagrams for the phase change from $156\text{-Co}_3\text{Br}_8$ to $12\text{-Co}_3\text{Br}_8$. The phonon spectra of (b) $164\text{-Co}_3\text{Cl}_8$ and $164\text{-Co}_3\text{Br}_8$.

Magnetic properties

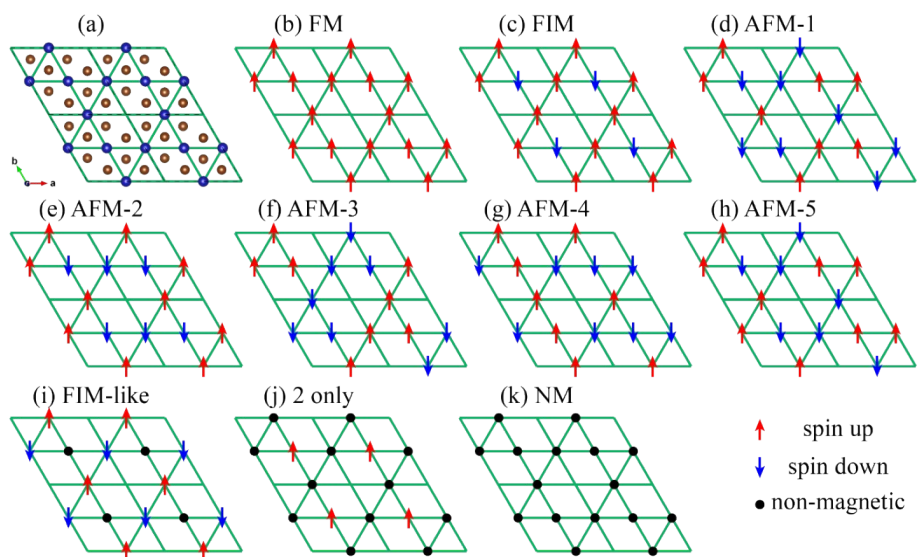


Figure S8. Magnetic configurations of 156- and 12- Co_3X_8 tested in the DFT calculation.

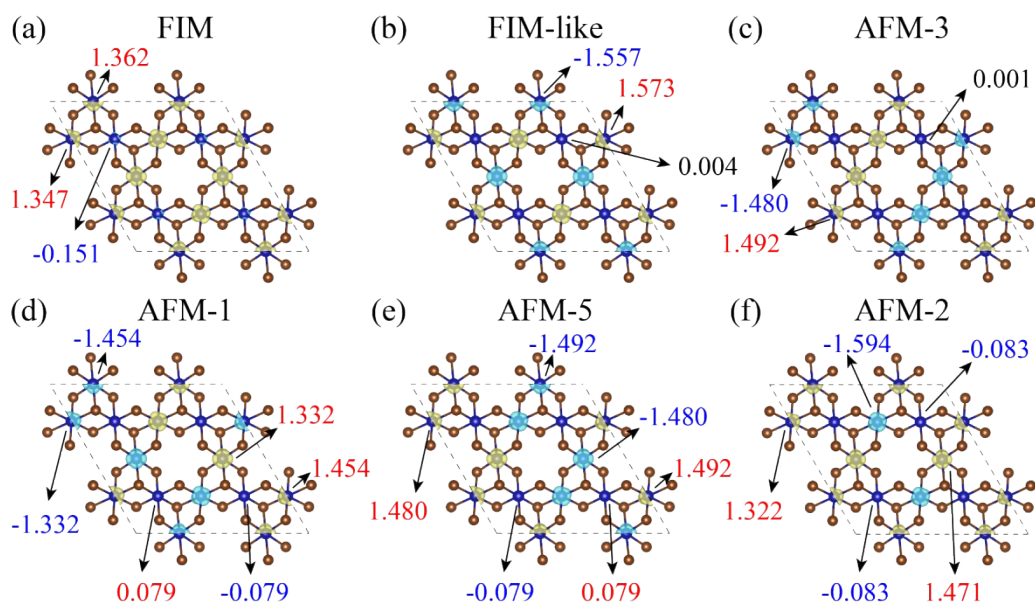


Figure S9. Spin density and magnetic moments of (a) FIM, (b) AFM-like, (c) AFM3, (d) AFM1, (e) AFM5, and (f) AFM2 12- Co_3Br_8 . The yellow and cyan denotes spin-up and spin-down, respectively. The isosurface is $0.02 \text{ e}/\text{\AA}^3$. The magnetic moments of some ions are marked.

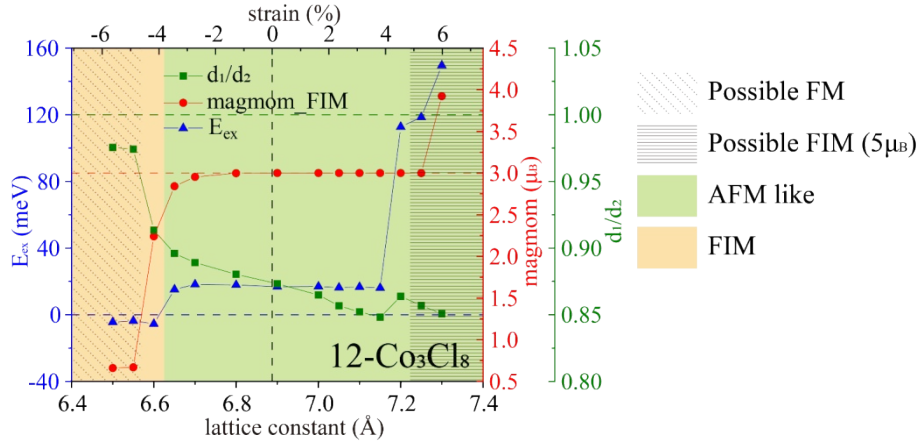


Figure S10. Strain-dependent magnetic properties of $12\text{-Co}_3\text{Cl}_8$. E_{ex} is defined as $E_{\text{ex}} = E_{\text{FIM}} - E_{\text{FIM-like}}$.

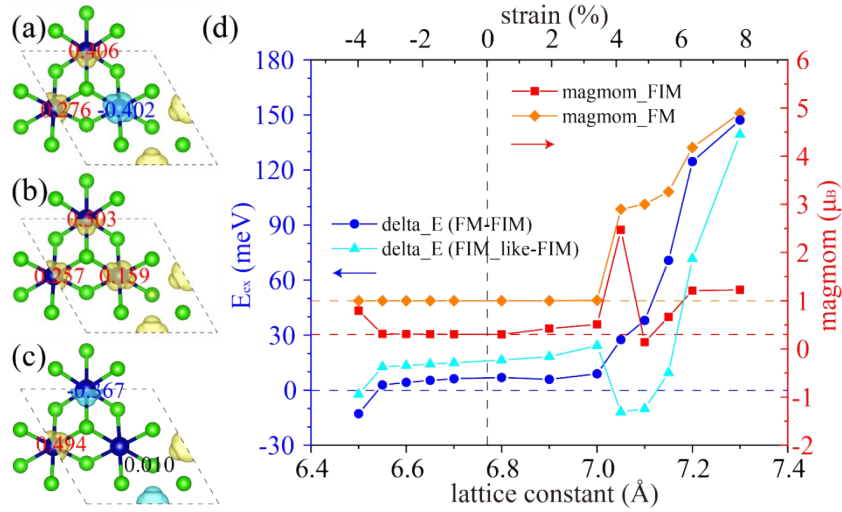


Figure S11. The spin density of (a) FIM, (b) FM, and (c) FIM-like $156\text{-Co}_3\text{Cl}_8$. The numbers are the magnetic moments. (d) Strain-dependent magnetic properties of $156\text{-Co}_3\text{Cl}_8$.

Electronic properties

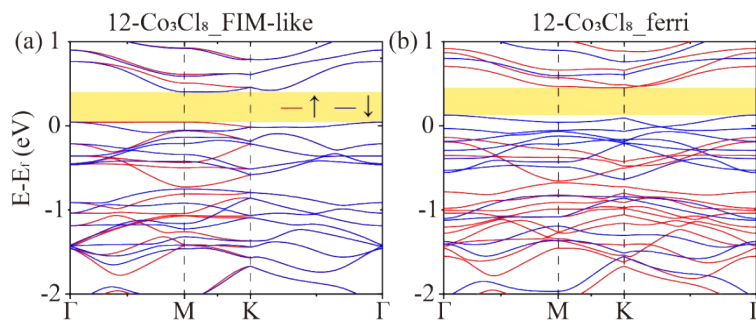


Figure S12. The band structures of $12\text{-Co}_3\text{Cl}_8$.

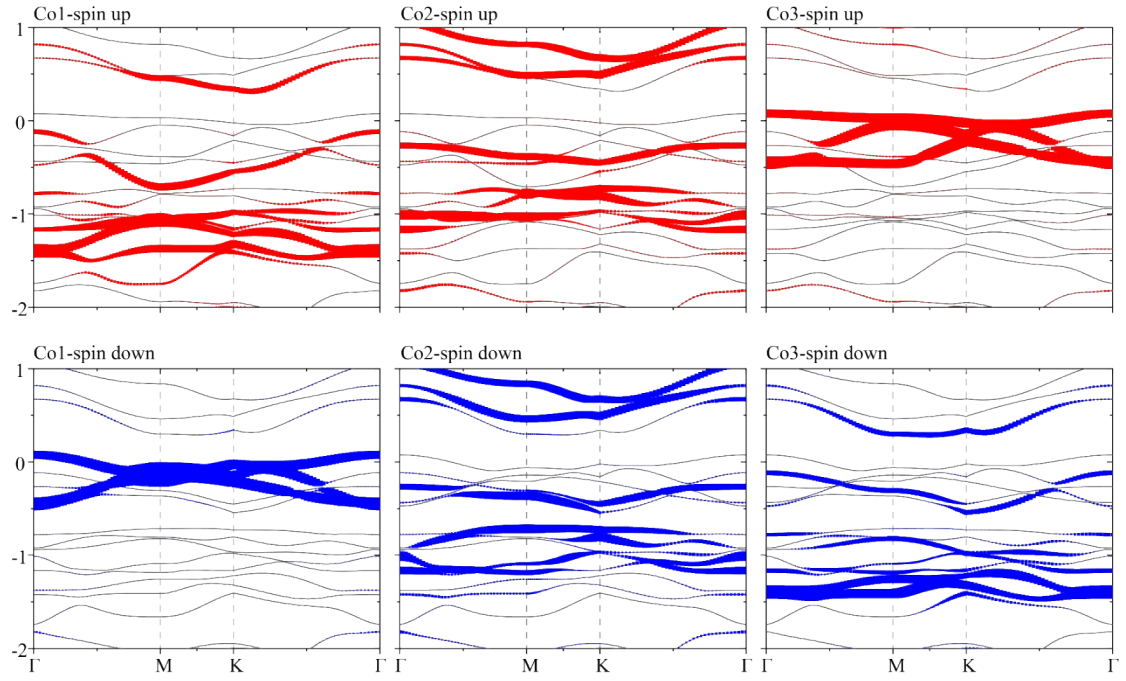


Figure S13. The pbands of Co1, Co2, and Co3 in $12\text{-Co}_3\text{Br}_8$.

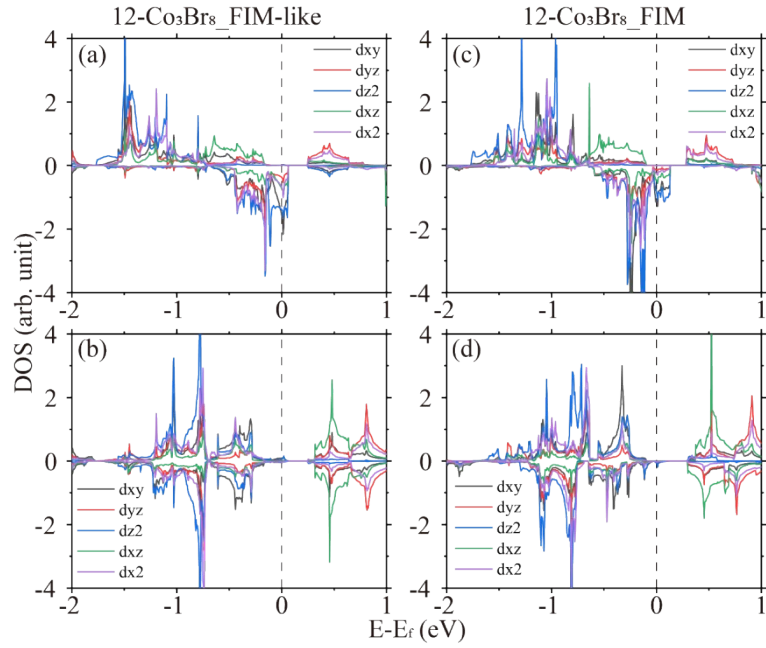


Figure S14. The PDOSs for $12\text{-Co}_3\text{Br}_8$: (a) Co1 and (b) Co2 in the FIM-like state, and (c) Co1 and (d) Co2 in the FIM state.

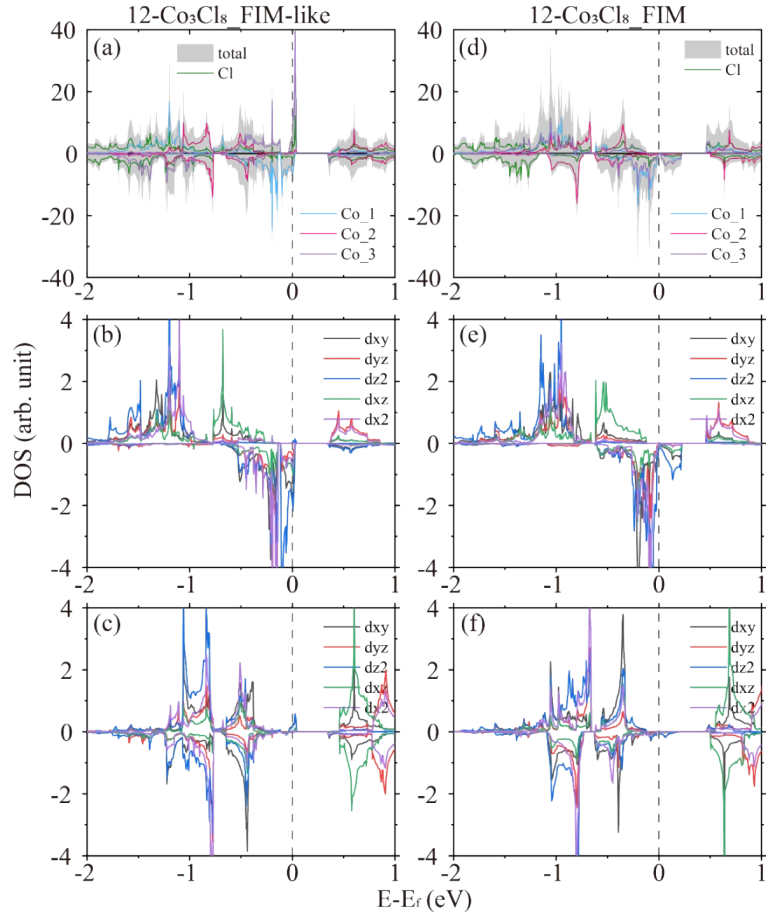


Figure S15. The PDOSs for 12- Co_3Cl_8 : (a) elements, (b) Co1 and (c) Co2 in the FIM-like state, and (d) elements, (e) Co1 and (f) Co2 in the FIM state.

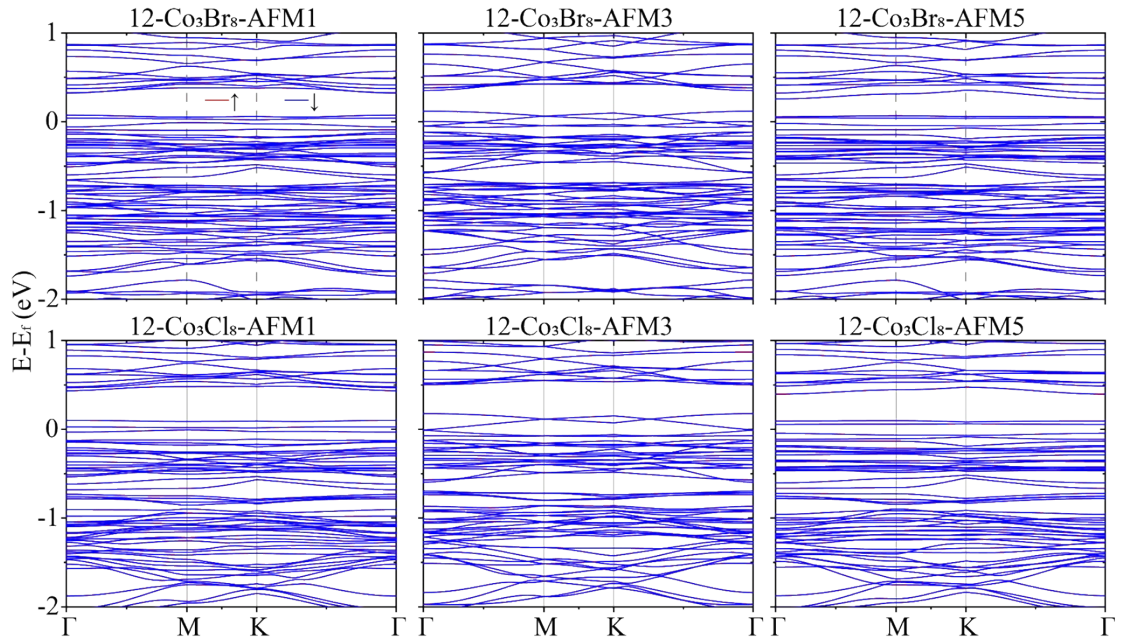


Figure S16. Band structures of AFM 12- Co_3X_8 .

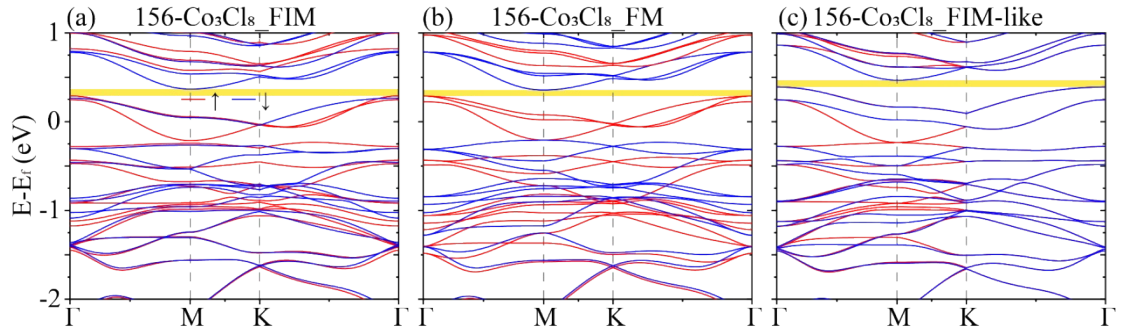


Figure S17. The band structures of (a) FIM, (b) FM and (c) FIM-like $156\text{-Co}_3\text{Cl}_8$.

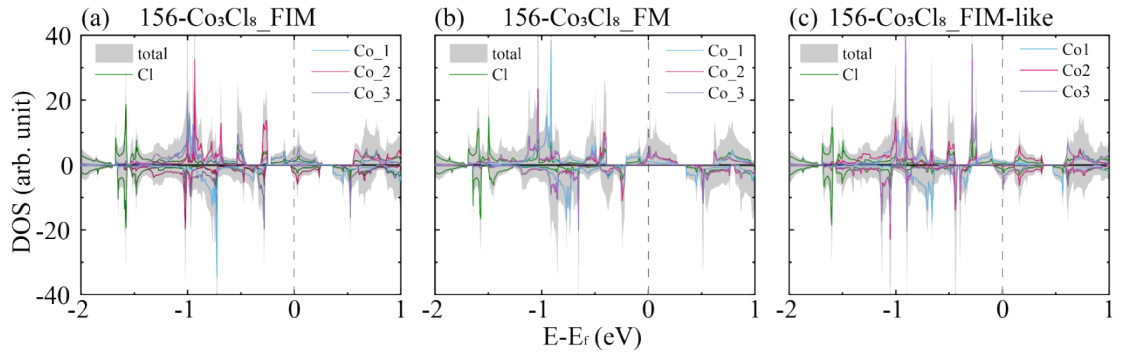


Figure S18. The PDOSs of (a) FIM, (b) FM and (c) FIM-like $156\text{-Co}_3\text{Cl}_8$.

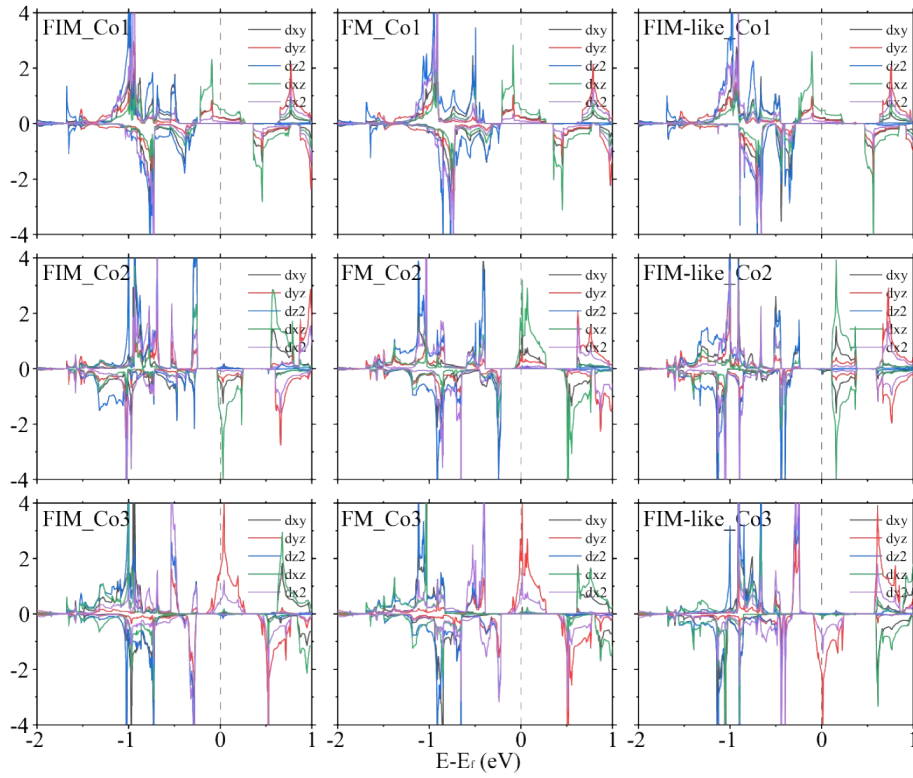


Figure S19. The PDOSs of three Co atoms in $156\text{-Co}_3\text{Cl}_8$ with different magnetic states.

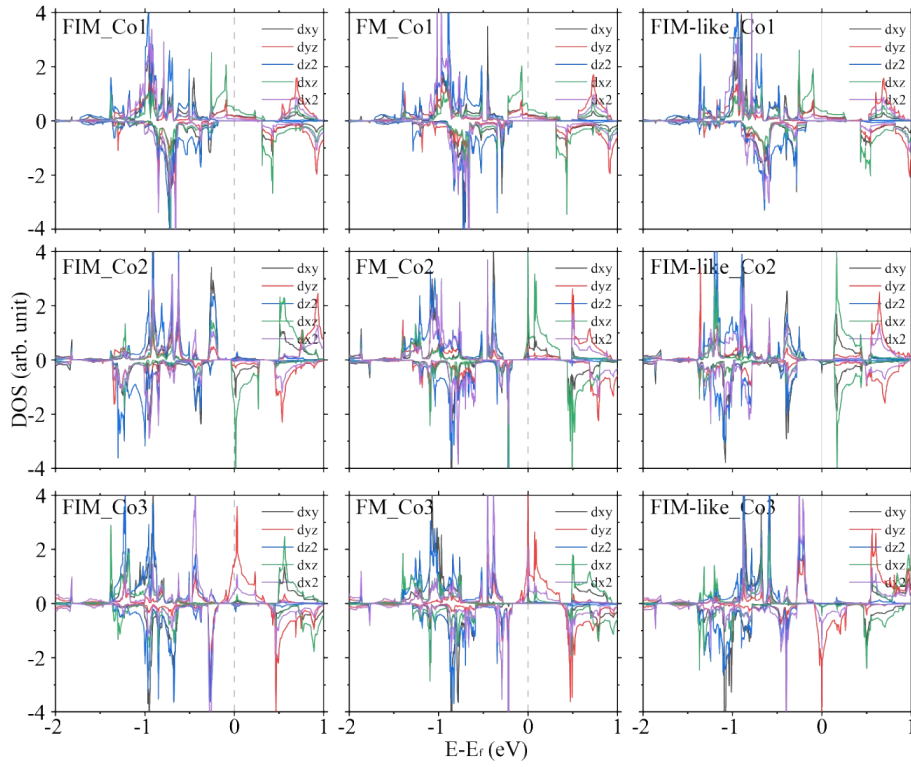


Figure S20. The PDOSs of three Co atoms in $156\text{-Co}_3\text{Br}_8$ with different magnetic states.

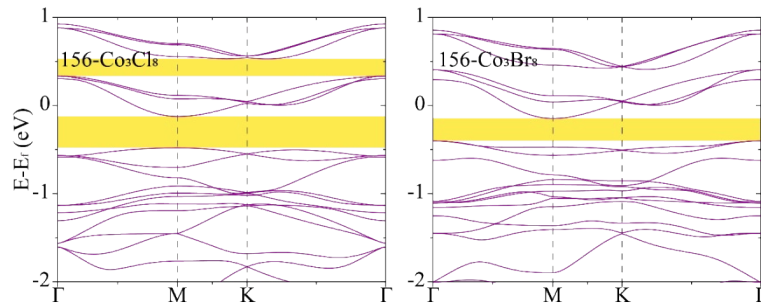


Figure S21. The band structures of $156\text{-Co}_3\text{X}_8$ without considering spin.

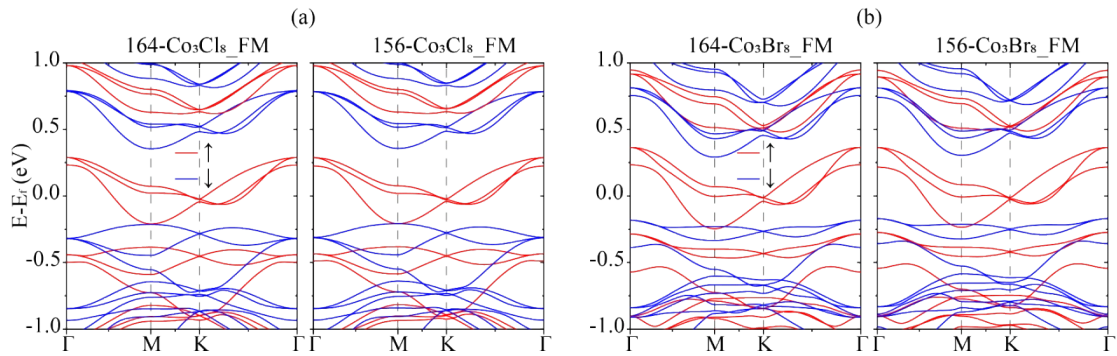


Figure S22. The comparison of band structures for 164- and $156\text{-Co}_3\text{X}_8$.

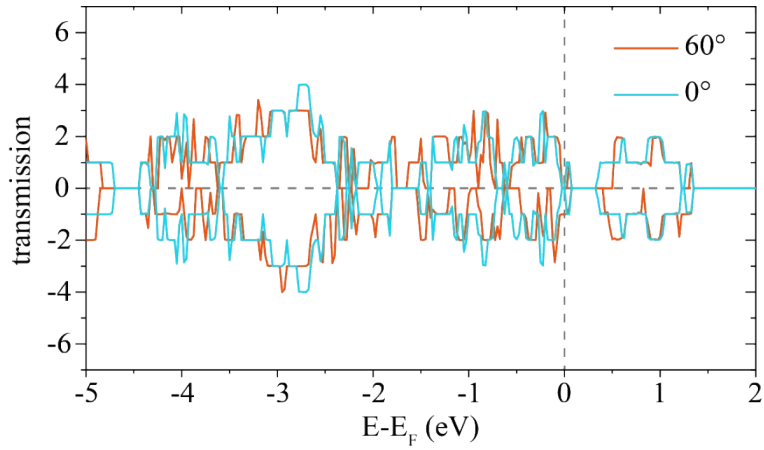


Figure S23. Spin-resolved transmission spectra of $12\text{-Co}_3\text{Br}_8$ under the 60° and 0° directions.

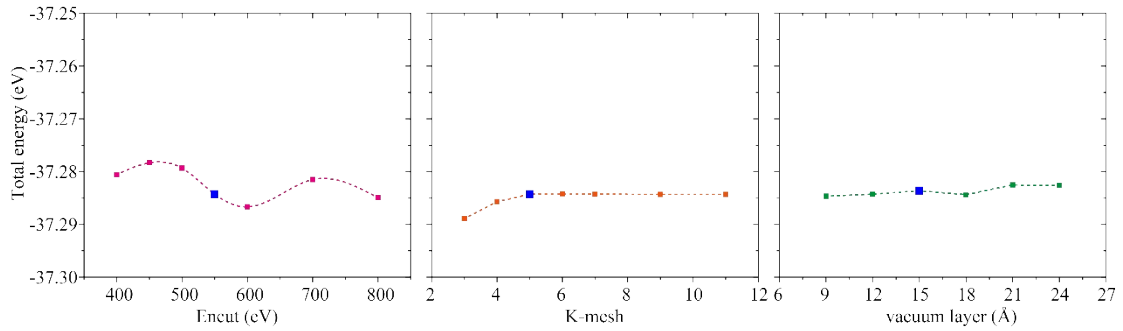


Figure S24. Convergence test for structure optimization. The total energy as a function of: (a) cut off energy, (b) K-mesh along xy plane, and (c) thickness of vacuum layer. The K-mesh in (a) and (c) are set as $5 \times 5 \times 1$, cut off energy in (b-c) are set as 550 eV, and vacuum layer in (a-b) are set as 15 Å. The condition used in our calculations is marked in blue blocks.